Journal of Catalysis **211,** 308–315 (2002)
doi:10.1006/jcat.2002.3729

Catalyst–Support Interaction in Fluorinated Carbon-Supported Pt Catalysts for Reaction of NO with NH_3

Weizhu An, Karl T. Chuang,[1] and Alan R. Sanger

Department of Chemical and Materials Engineering, University of Alberta, Edmonton, Alberta, Canada T6G 2G6

Received January 7, 2002; revised June 5, 2002; accepted June 27, 2002

Catalysts comprising Pt supported on fluorinated carbon (0, 10, 28, and 65% F) have been characterized and their activities have been compared for reaction of NO with NH_3. Both catalytic activity and selectivity to formation of N_2 over FC-supported Pt catalysts vary with fluorine content. Activity and selectivity each increased with increasing F content to a maximum value at 28% F, then each deteriorated for Pt supported on FC with 65% F. Selectivity to N_2 over FC-supported catalysts at temperatures below 200°C is superior to that at higher temperatures. XPS showed that Pt was situated at surface sites neighboring fluorinated carbons for FC having 0–28% F. However, Pt is enveloped in the support with 65% F. A positive shift of F 1s and a negative shift of Pt 4f binding energy were detected after Pt was deposited on the FC supports, indicating that electron charge transfer from F to Pt occurred on surfaces of FC-supported Pt catalysts. The increase in selectivity with FC-supported Pt catalysts is attributed to the electronic interaction between FC and Pt, which enhanced dissociative chemisorption of NO on active Pt sites.

Key Words: **fluorinated carbon; Pt; catalyst-support interaction; reaction of NO with NH_3.**

INTRODUCTION

Selective catalytic reduction (SCR) of NO with NH_3 is a component reaction of well-established postcombustion technology for the removal of NO_x from stationary sources and chemical plants (1–4). Although V_2O_5/TiO_2-based catalysts have been commercialized as medium-temperature (300–450°C) $DeNO_x$ catalysts, there still exist challenges and opportunities to further extend the operation temperature window toward lower (150–300°C) and higher (up to 600°C) operating temperatures to meet the needs of different industrial applications (4–6).

Precious metals, in particular Pt-based catalysts, are well-known low-temperature $DeNO_x$ catalysts; however, they are also notorious for high selectivity to N_2O formation and for having a narrow operating-temperature window, which has significantly limited their commercial application (2). Studies on oxide-supported Pt catalysts for SCR of NO with hydrocarbons have shown that both selectivity and activity of supported Pt catalysts are influenced by the interaction between Pt and support materials. The ratio of N_2/N_2O formation has been modified by varying the ratio of SiO_2/Al_2O_3 of ZSM-5-supported Pt and noble metal catalysts when propene was used as reducing agent (7, 8). It has also been reported that only selectivity was affected by the ratio of SiO_2/Al_2O_3 in ZSM-5-supported Pt catalysts when NH_3 was used as reducing agent (7). The participation by catalyst support material in the reduction of NO over these supported catalysts and/or promotion of the catalyst by the support are evident.

The combination of two nitrogen atoms on the surface of an active catalytic site to form N_2 is an essential step in the $DeNO_x$ process. It has been shown that one of the nitrogen atoms in product N_2 is from the dissociation of NO and the other is from NH_3, and that chemisorbed molecular NO coupled with a nitrogen from NH_3 to form N_2O over Pt-based catalysts when ammonia was used as reducing agent (5, 9).

Modification of the chemical environment of Pt as the active component through an electronic interaction between metal and support/promoter can significantly change the activity and selectivity of supported Pt catalysts. An increase of catalytic activity by two orders of magnitude and selectivity by four times was reported for SCR of NO with propene when Na was introduced into a Pt/Al_2O_3 catalyst. The remarkable promotion of activity and selectivity effected by Na addition was attributed to the electronic interaction between Na and Pt, which enhanced the dissociative chemisorption of NO on Pt (10).

Fluorinated carbon (FC) is produced by reaction of carbon with fluorine (11). The electronegativity difference between F (4.0) and C (2.5) and the high fluorine concentration at the carbon surface give rise to unique physicochemical properties of FC, such as strong hydrophobicity and a variety of types of C–F bonds (12–14). The nature of the complex chemical bonds in FC, including ionic, semiionic, and covalent bonds between carbon and fluorine, has been the subject of intensive study (12–16). However, few studies

[1] To whom correspondence should be addressed. Fax: (780) 492-2881. E-mail: KarlT.Chuang@ualberta.ca.

0021-9517/02 $35.00

have examined the effect of the electronic interactions between carbon and fluorine in FC on the performance of active metal catalyst when FCs are used as catalyst supports. Our preliminary study on SCR of NO with NH_3 showed that catalytic activity and water resistance were both improved over a FC (28%)-supported Pt catalyst compared to that of the fluorine-free activated carbon (AC)-supported Pt catalyst (17). It was proposed that the electronic interaction between FC and Pt was an important factor influencing the surface reaction of NO with NH_3.

In the present study, a series of FC (F content of 0, 10, 28, and 65%)-supported Pt catalysts were examined for SCR of NO with NH_3. The focus was on improved understanding of the electronic interaction between Pt and FC. Although numerous studies have been devoted to XPS characterization of various fluorinated carbon materials, XPS data on FC-supported metal catalysts have not previously been described. Herein, it will be shown that the catalytic activity and selectivity of reaction of NO with NH_3 over FC-supported Pt catalysts are affected by the electronic interaction between FC and Pt.

EXPERIMENTAL

Catalyst Preparation

Preparation of Pt/FC catalysts. Commercially available fluorinated carbons (FCs) with fluorine content of 10, 28, and 65%, herein designated FC-10, FC-28, and FC-65, respectively, are manufactured by fluorination of carbon black. In this study, these FC (Allied Signal Corp.) were used as support material for Pt/FC catalysts . For comparison purposes, fluorine-free carbon black from Lodestar (designated FC-0) and a commercial activated carbon from Aldrich (designated AC) also were used as catalyst supports. A 4% Pt solution of tetra-ammine platinum(II) nitrate (Colonial Metals Inc.) in water was used as Pt catalyst precursor. The procedures for the preparation of FC-supported Pt catalysts are described elsewhere (17). Briefly, the desired amount of platinum-containing solution was first added to a mixture of 50 wt% methanol in water, and then FC powder or AC powder was added. After thorough mixing for 30 min, the mixture was reduced to dryness in a rotary evaporator under an infrared light. The supported Pt catalyst was reduced in flowing H_2 at 300°C for 14 h.

The BET surface area and pore distribution of Pt/FC and Pt/AC catalysts are presented in Tables 1 and 2.

Preparation of Pt/FC/ceramic catalysts. To model hydrophobic catalysts suitable for industrial applications, the Pt/FC catalysts, and for comparison a Pt/AC catalyst, were coated onto ceramic rings, as described previously (17). The catalyst-coated ceramic rings were then calcined at 300°C in air for 3 h. The Pt/FC/ceramic catalysts thus prepared each contained 0.1 wt% Pt. The Pt/FC/ceramic catalysts were then crushed and sieved to 9–20 mesh particles (~0.833–1.981 mm) for activity testing using a laboratory-scale reactor.

TABLE 1

Physical Characterization of FC- and AC-Supported Pt Catalysts

Samples	BET (m^2/g)	BET of the support (m^2/g)	Metal or particle diameter (nm)	Dispersion of Pt by XRD (%)	Dispersion of Pt by chemisorption (%)
10 wt% Pt/FC-0	184	216	14.8	7.3	16.5
10 wt% Pt/FC-10	188	199	16.3	6.6	7.2
10 wt% Pt/FC-28	157	154	15.9	6.8	2.1
10 wt% Pt/FC-65	291	359	20.3	5.3	0.9
10 wt% Pt/AC	1472	1754	4.1	26.2	22.5

Catalyst Characterization

The surface area (Table 1) and pore size distributions (Table 2) of FC- and AC-supported Pt catalysts were measured by nitrogen adsorption using an Omnisorp 360 analyzer (21). The mean particle size of Pt in the FC-supported Pt catalyst was determined by XRD (Philips X-Ray Diffractometer, PW 1730, Holland Philips), based on the broadening of the platinum XRD peak at 39.8° (2θ) (21). Pt dispersions were measured by both XRD and H_2 pulse chemisorption (Table 1). The electronic interactions between F and C in the FC supports and between FC and Pt were studied using XPS (SSX-100, Al $K\alpha$ X rays) (Tables 3 and 4). The scans were obtained using a 600-μm spot size and 150-eV pass energy. High-resolution scans were taken with a 600-μm spot size and 50-eV pass energy. All powder samples were mounted by pressing them onto indium foil before measurements.

TABLE 2

Pore Distribution of FC- and AC-Supported Pt Catalysts

Pore radius (nm)	Pore volume (mL/g)[a]				
	10 wt% Pt/FC-0	10 wt% Pt/FC-10	10 wt% Pt/FC-28	10 wt% Pt/FC-65	10 wt% Pt/AC
>30	0 (0.04107)	0 (0.1082)	0 (0.01367)	0.003 (0.03714)	0 (0)
30–20	0.01749 (0.05817)	0.03939 (0.07458)	0.04372 (0.03143)	0.04417 (0.03218)	0.01416 (0.00822)
20–10	0.08064 (0.1397)	0.1177 (0.1580)	0.1203 (0.07186)	0.1253 (0.08908)	0.07347 (0.08832)
10–5	0.08049 (0.0975)	0.1079 (0.1189)	0.1008 (0.03251)	0.1109 (0.08999)	0.1871 (0.2491)
5–1	0.04977 (0.04811)	0.0583 (0.0525)	0.0519 (0)	0.1129 (0.09715)	0.5848 (0.6988)

[a] Numbers in parentheses are pore volumes for fresh supports.

TABLE 3

XPS Data for Supports and Supported Pt Catalysts

Sample	Elements detected (atomic percent)			
	Carbon	Oxygen	Fluorine	Platinum
FC-0	99	0.7	0.0	0.0
FC-10	79	1.0	20	0.0
FC-28	80	2.4	18	0.0
FC-65	53	<0.1	47	0.0
10 wt% Pt/FC-0	98	1.7	0.0	0.4
10 wt% Pt/FC-10	94	1.8	3.8	0.4
10 wt% Pt/FC-28	87	1.7	11	0.2
10 wt% Pt/FC-65	34	0.5	66	<0.1[a]

[a] No surface Pt detected by XPS.

High-resolution XPS depth-profile analysis for the Pt/FC-65 catalyst was performed using synchrotron radiation (Scienta 100 electron energy analyzer); the pressure in the chamber was 1.3×10^{-10} Torr.

Catalytic Activity and Selectivity Measurement

Reaction of NO with NH_3 over the FC- and AC-supported Pt catalysts was carried out in a quartz reactor, as described previously (17). Briefly, the reactor consists of preheating, reaction, and cooling zones. The Pt/FC/ceramic catalyst was packed inside the reaction zone (8-mm ID and 100 mm long). Reactant gases were fed into the preheating zone through three separate tubes and mixed at the top of the reaction zone. The feed gas was prepared by blending individual gases using mass flow controllers. A typical initial volumetric gas composition was 500 ppm NO, 500 ppm NH_3, 4% O_2, and balance N_2. A total gas flow rate of 600 mL/min (STP) corresponding to a gas hourly space velocity of 14,400 h^{-1} was used throughout this study.

Gas Analysis

NO and NO_2 concentrations were analyzed using a chemiluminescence NO/NO_x analyzer (Thermo Electro Corp., Model 10). NO_2 concentration was determined from the difference between NO_x and NO measured using the NO/NO_x analyzer. To eliminate the interference of NH_3 on NO_x analysis, an ice-bath trap containing boric acid solution was used to remove NH_3 before effluent gas was fed to the NO/NO_x analyzer. An online gas chromatograph (HP 5809II) equipped with a Porapak R column and TCD was used for N_2O analysis. A separate sample line was used for ammonia analysis. Ammonia concentration was determined using standard titration methods and hydrochloric acid solution as titrant.

TABLE 4

Binding Energy Change of Pt $4f_{7/2}$ for Fluorinated-Carbon-Supported Pt Catalysts

Sample	Platinum ($4f_{7/2}$)
10 wt% Pt/FC-0	71.6 eV[a], metallic
10 wt% Pt/FC-10	71.5 eV, metallic
10 wt% Pt/FC-28	71.4 eV, metallic
10 wt% Pt/FC-65	No surface Pt detected

[a] Binding energy referenced to carbon (1s) at 284.5 eV.

RESULTS AND DISCUSSION

Physical and Structural Characterization of Supported Pt Catalysts

The physical properties of FC- and AC-supported Pt catalysts characterized by XRD and BET methods are listed in Table 1. Depositing Pt onto the carbon support caused a decrease of BET surface area (Table 1), except for FC-28, where the BET surface area of the catalyst was substantially similar to that of the support alone. The Pt-induced decrease of BET surface area is attributed to pore blocking by Pt particles. The average Pt particulate size (Table 1) was comparable to the size of the average support pore (Table 2). The growth of Pt particles in or at the openings to pores reduced access and thereby reduced total accessible pore volume as well as the average pore size measured for Pt/FC, compared with values for the supports alone.

Accessibility of aqueous solution of the Pt precursor to pores was affected by the F content, resulting in changes to pore-size distributions as follows. A decrease in pore volume of all pores was observed when Pt was deposited on the support having low fluorine content (FC-10) and fluorine-free carbons (FC-0 and AC). In contrast, the pore volume of medium and small pores (radius < 30 nm) increased as the pore volume of larger pores decreased when Pt was deposited on moderate and high fluorinated carbons (FC-28 and FC-65). This effect is attributed to differences in accessibility to pores by the water-containing solution. As the fluorine content of the support increased, the fluorinated carbon became more hydrophobic. Consequently, the water-containing Pt solution was less able to access and occupy medium and small pores. Hence, Pt particles were more likely to grow and accumulate on the outer surface or in larger pores, resulting in larger particle size and lower dispersion (Table 1). Thus Pt dispersion decreased with increasing fluorine content in the FC supports.

Pt dispersion was also measured by hydrogen chemisorption (Table 1). Surprisingly, apparent values for Pt dispersions measured by hydrogen chemisorption were significantly lower than values measured by XRD for the fluorinated-carbon-supported Pt catalysts, especially when using the two most fluorinated supports (FC-28 and FC-65). These two catalysts showed very low ability to chemisorb hydrogen. Suppression of chemisorption of hydrogen

indicated that there existed a strong interaction between Pt and fluorinated carbon in fluorinated-carbon-supported Pt catalysts. The catalyst–support interaction in Pt/FC-65 was so strong that catalytic activity was inhibited (see Effect of F Content on Catalytic Activity and Selectivity).

XPS Study of the Interactions between Fluorine and Carbon and between Pt and FC Support

Table 3 presents the XPS data for FC supports and the corresponding supported Pt/FC catalysts. Deposition of Pt onto FC increased the proportion of surface carbon atoms from 79 to 94% and from 80 to 87% for FC-10 and FC-28, respectively, and decreased surface carbon atoms from 53 to 34% for FC-65. The proportion of surface fluorine atoms decreased from 20 to 3.8% and from 18 to 11% for FC-10 and FC-28, respectively, but increased from 44 to 66% for FC-65. Further, the proportion of Pt surface atoms detected by XPS decreased with increasing fluorine content of the support, even though each had the same 10 wt% Pt loading. Surprisingly, virtually no surface Pt was detected by XPS for the sample Pt/FC-65 containing 10 wt% Pt. By calculating the atomic ratio of fluorine to carbon on the surface of FC-supported Pt catalysts before and after incorporation of Pt, it was found that the ratio of surface F to surface C dropped from 0.25 to 0.04 for FC-10 and from 0.23 to 0.13 for FC-28, but increased from 0.83 to 1.94 for FC-65. Thus Pt/FC-10 and Pt/FC-28 were shown to have a relatively fluorine-lean surface, and Pt/FC-65 was shown to have a relatively fluorine-rich surface. These data show that Pt was situated at fluorine-rich sites and covered a significant fraction of F sites of FC-10 and FC-28.

Hydrogen chemisorption behavior was a function of both the availability of Pt sites on the catalyst surface and the Pt-support interaction (19). The low proportion of surface Pt sites for Pt/FC-28 and Pt/FC-65 detected by XPS was consistent with the observed low hydrogen chemisorption ability. For Pt/FC-28, the loss of hydrogen chemisorption ability is attributed directly to the interaction between fluorine and Pt. The XPS and hydrogen chemisorption data each appeared to show that very few Pt surface sites were present on 10 wt% Pt/FC-65. The loss of hydrogen chemisorption ability for this material is exacerbated by the envelopment of Pt by FC-65, as will now be described.

To determine the location of Pt in Pt/FC-65, synchrotron radiation was used to perform high-resolution XPS depth-profile analysis of Pt/FC-65. The depth profile clearly showed that the large majority of Pt was not on the surface, and Pt particles were located mainly about 1 nm below the surface (Fig. 1). The results from XPS depth-profile analysis were consistent with a structure in which Pt sites were enveloped within perfluorinated carbon. A similar metal–support interaction effect was observed for the Pt/TiO_2 system (19, 20). The suppression of H_2 and CO chemisorption on Pt/TiO_2 in a strong metal–support interaction (SMSI)

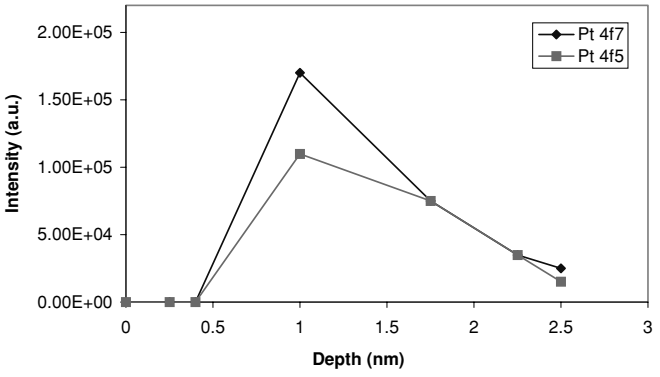

FIG. 1. Depth profile for 10 wt% Pt/FC-65.

state was explained by site blockage due to the migration and formation of a TiO_x overlayer. The overlayer of FC-65 on Pt as shown by depth-profile analysis accounts for both the exceptionally low amount of H_2 chemisorption and the weak XPS Pt signal observed for highly fluorinated-carbon-supported Pt catalysts, especially Pt/FC-65. However, it is unknown how and during what preparation stage these perfluorinated carbon species enveloped the Pt particles. Such behavior is unprecedented for metal–FC systems.

XPS spectra of the fluorinated carbon supports are compared with spectra of the corresponding supported Pt catalysts in Figs. 2 and 3 (C 1s), and 4 and 5 (F 1s), respectively. C 1s spectra initially changed with increasing F content, from one peak to two main peaks, and then to

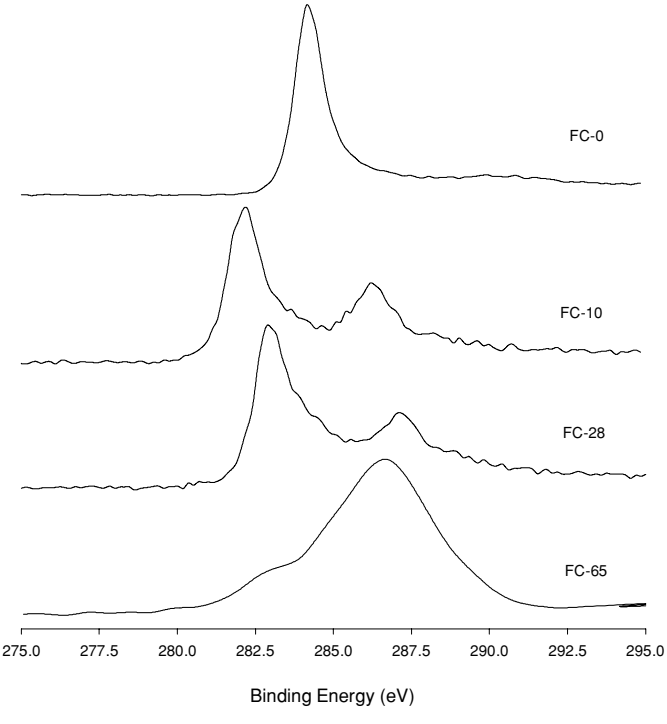

FIG. 2. C 1s XPS spectra of fluorinated carbon.

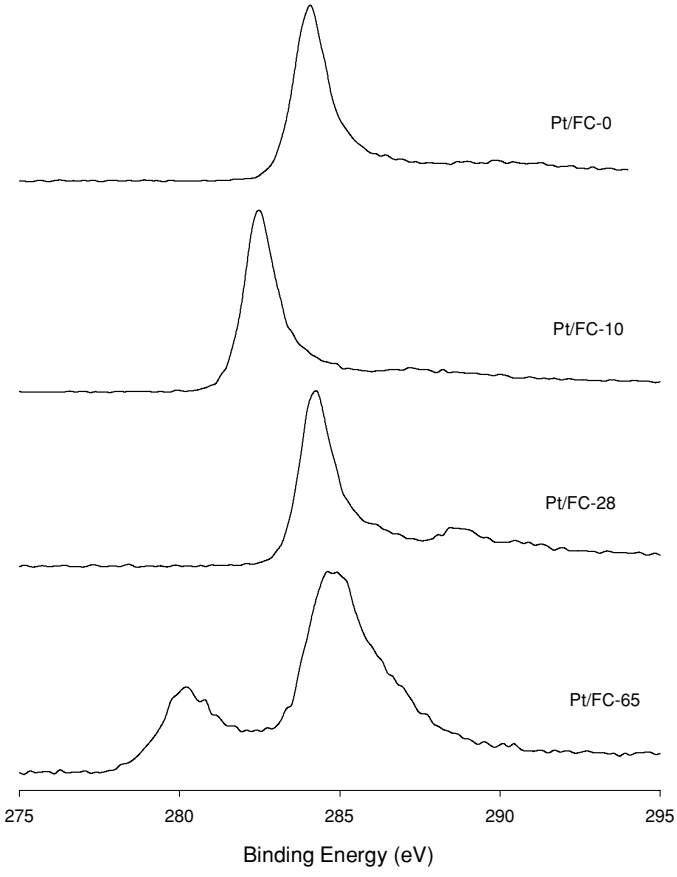

FIG. 3. C 1s XPS spectra of FC-supported Pt catalysts.

one charge-broadened peak (Fig. 2). For fluorine-free carbon, FC-0, there was only one peak, located at 284.5 eV, corresponding to nonfluorinated graphitic carbon having only C–C bonds. For each FC, the peak located at lower binding energy (BE) is assigned to nonfluorinated carbon, "graphitic carbon," and the peak at higher value is assigned to C atoms bonded to F atoms (16). Before Pt is deposited, the peak C 1s binding energy for envelopes assigned to C bonded directly to F increased slightly as F content increased (Fig. 2). The main C 1s spectra at binding energies of 286.2 ± 0.3 and 287 ± 0.3 (shoulder) eV for FC-10 and 287.2 ± 0.3 eV for FC-28 are assigned to C̲–CF and C̲–F with significant semiionic bonding character. The corresponding F 1s components were observed at 685.6 and 686.2 eV (Fig. 4). For FC-65, the broad C 1s and F 1s envelopes indicated that a wide range of F–C bonding existed in this support, including covalent C–F bonds in the α position of border CF_2 groups and other CF_n groups. The F 1s peak became broader with increasing fluorine content. The F 1s spectra of FC-65 showed an asymmetric broad peak from 680 to 689 eV. Deconvolution of the broad envelop of F 1s peaks for FC-65 indicated that several C–F components were present, including three major components, with binding energies of 687.26, 685.70, and 683.67 eV. Generally, the binding energy of fluoride anions in solids has been found to vary with environment between 683 and 685 eV (12). It is well accepted (12, and references therein) that the nature of the bond between F and C changes with fluorine content in fluorinated carbons. The values for FC-10, FC-28, and FC-65 each showed that a proportion of C–F bonds had strong ionic character. When the F/C atomic ratio is low, the C–F bond has significant ionic character. As the fluorine content increases, the nature of the C–F bonds changes from mainly ionic to semiionic and then to covalent.

The C 1s and F 1s spectra for Pt/FC catalysts are shown in Figs. 3 and 5. After depositing Pt onto FC, the C 1s spectrum for Pt/FC-0 had the same binding energy as FC-0 alone, indicating that no major electronic interaction occurred between Pt and carbon in this sample. For FC other than FC-0, the C 1s spectra for Pt/FC differed from the spectra for the corresponding FC alone. The C 1s components corresponding to C̲–F (higher binding energy) decreased for the two high-fluorine-content samples, Pt/FC-28 and Pt/FC-65, and was not detected for Pt/FC-10. The C 1s spectra for Pt/FC-65 split into two broad peaks. The lower binding energy component can be assigned to both C̲–C and C̲–H bonded carbon, while the higher binding energy component appeared to contain signals from C̲–F bonded carbon (Fig. 3). The decrease or disappearance of signals attributed to carbon having C–F bonds on the surface of Pt/FC-10 and Pt/FC-28 samples paralleled the corresponding reductions in F 1s signals for FC-10 and FC-28 (Fig. 5). In contrast to Pt/FC-10 and Pt/FC-28 samples, the F 1s spectra of Pt/FC-65 showed two peaks, a broad peak at lower binding energy and another peak as a shoulder at higher binding energy. It was also noted that the binding energy of residual F 1s components

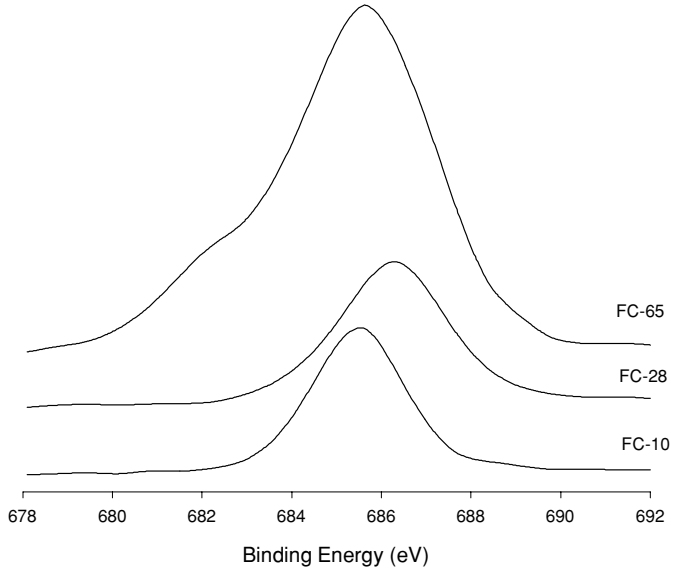

FIG. 4. F 1s XPS spectra of fluorinated carbon.

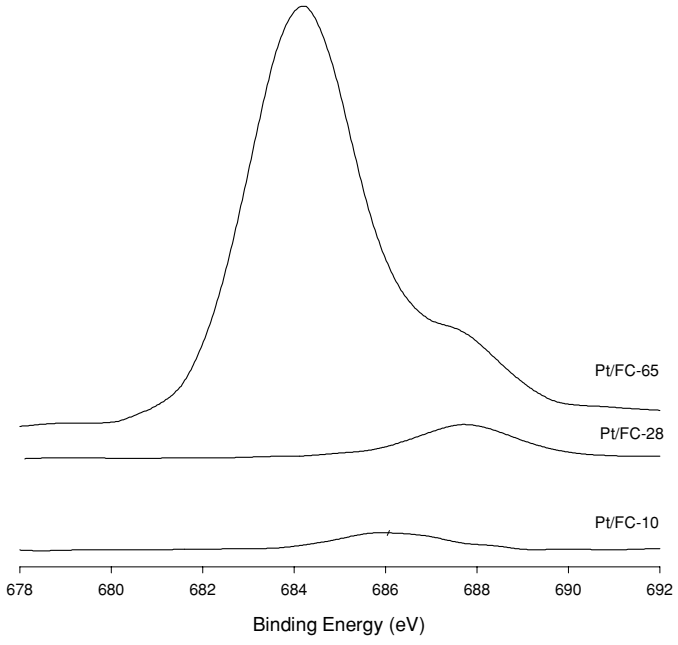

FIG. 5. F 1s XPS spectra of FC-supported Pt catalysts.

corresponding to C–F bond shifted positively with increasing F content. The disappearance or decrease of signals for carbon having C–F bonds for Pt/FC-10 and Pt/FC-28 catalysts showed that Pt was situated at fluorinated carbon sites. For Pt/FC-10 and Pt/FC-28, almost all fluorinated carbon domains were covered with Pt, and all Pt particles were closely in contact with fluorinated carbon species on the surface of the Pt/FC samples. The positive shift of F 1s binding energy with increasing F content also indicated the occurrence of electron charge transfer from F to Pt when Pt was deposited onto those surface fluorinated carbon sites.

Table 4 shows the Pt $4f_{7/2}$ binding energy for each Pt/FC. The Pt $4f_{7/2}$ binding energy decreased by −0.2 eV as fluorine content increased from 0 to 28%. The negative shift of binding energy for FC-supported surface Pt atoms confirmed that electronic interactions existed between FC and Pt atoms. The electronic perturbation of Pt active sites by FC parallels the observed suppression of hydrogen chemisorption on Pt/FC-supported catalysts. Surprisingly, the fluorine content on the surface of Pt/FC-65 increased from 47 to 66% after depositing Pt, and almost no Pt was found on the surface. Thus, the support was restructured as a consequence of Pt deposition. It may be concluded that both electronic interaction between Pt and FC and the active site blockage by FC are responsible for the suppression of H_2 chemisorption and lower catalytic activity (see below).

Effect of F Content on Catalytic Activity and Selectivity

The impact of the electronic interaction between Pt and FC support on catalytic activity and selectivity for the reaction of NO with NH_3 has been examined using Pt catalysts having the same Pt loading on FC supports containing different amounts of fluorine (0, 10, 28, and 65 wt%), in the temperature range 100–275°C and at a constant space velocity of 14,400 h^{-1}. Neither CO_2 nor CO was detected in the effluent, using online GC. The catalytic activity and selectivity of Pt/FC catalysts showed a strong dependence on F content (Figs. 6 and 7). The Pt/FC series of catalysts showed higher catalytic activity than did Pt/AC, even though the latter had much higher Pt dispersion. Thus the reaction of NO with NH_3 over these catalysts was more sensitive to the Pt chemical environment than to catalyst structure, as previously reported for a related catalytic reaction system (21). For each catalyst, NO conversion increased with temperature, to a maximum value at temperatures in the range 175–200°C, and then decreased at temperatures over 200°C (Figs. 6 and 7). At temperatures below 200°C, catalysts supported on carbon with low-to-moderate F content (FC-10 and FC-28) showed greater low-temperature NO conversion than catalysts having FC-0, FC-65, or AC as supports. At 150°C, NO and NH_3 conversion over Pt/FC-28 catalyst were, respectively, about 2.5 and 3.0 times higher than that over Pt/FC-0 catalyst (Fig. 6).

Selective catalytic reduction of NO with NH_3 over supported Pt catalysts involves several interactions, of which

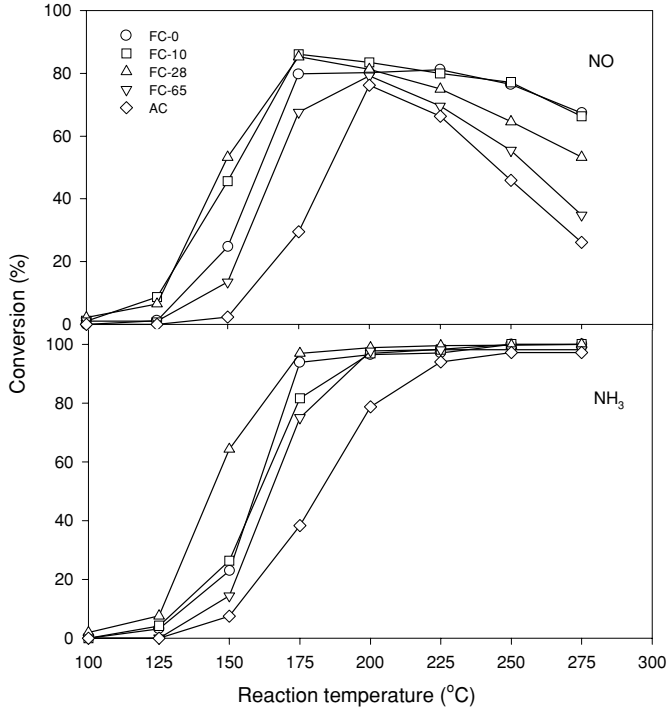

FIG. 6. Effect of fluorine content on activity for reaction of NO with NH_3 over Pt/FC and Pt/AC catalysts. Experiment conditions, initial gas composition: (NO) = 500 ppm; (NH_3) = 500 ppm; (O_2) = 4% (v/v); N_2 (balance); GHSV = 14,400 h^{-1}.

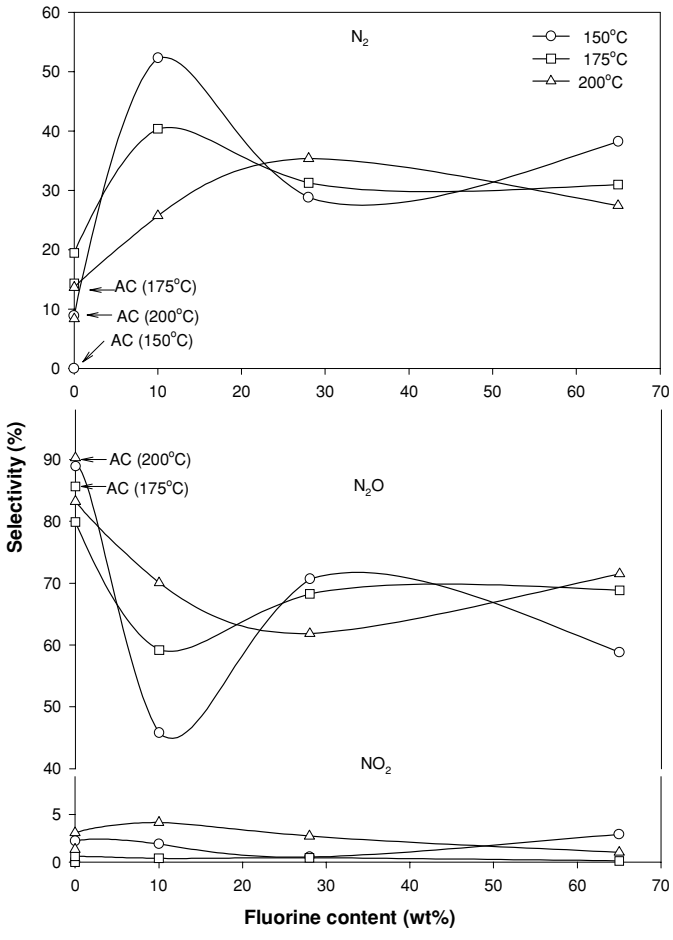

FIG. 7. Selectivity of reaction of NO with NH_3 over Pt/FC as a function of fluorine content.

the following are the main reactions (1, 2):

$$4NO + 4NH_3 + O_2 = 4N_2 + 6H_2O, \quad [1]$$

$$4NO + 4NH_3 + 3O_2 = 4N_2O + 6H_2O, \quad [2]$$

$$2NH_3 + 2O_2 = N_2O + 3H_2O, \quad [3]$$

$$4NH_3 + 3O_2 = N_2 + 6H_2O, \quad [4]$$

$$4NH_3 + 5O_2 = 4NO + 6H_2O. \quad [5]$$

The almost one-to-one consumption of NO and NH_3 and formation of both N_2 and N_2O as products over FC-supported catalysts at temperatures below 200°C indicated that Reactions [1] and [2] were dominant in this temperature range. The above XPS data showed that the F content affected both the F–C bonding and the Pt–FC electronic interaction. In combination, these data suggest that the optimum F content favored either or both Reactions [1] and [2], and excess F inhibited these reactions. The inhibiting effect of high F content in Pt/FC-65 is attributed to the blockage of surface Pt active sites by fluorinated carbon and perfluorinated carbon surface domains.

At temperatures above 200°C, the molar ratio of reacted NO to NH_3 became less than unity, as ammonia was more readily oxidized by oxygen at high temperatures (Reactions [3], [4], and [5]) (2, 22). Among the Pt/FC series of catalysts, NO conversion decreased with increasing fluorine content, indicating that the presence of fluorine also promoted NH_3 oxidation by O_2 to NO at temperatures above 200°C. The electronic interaction between fluorine and carbon resulted in a more positively charged carbon (XPS). Pt deposited onto the fluorinated carbon surface interacted with F sites (e.g., Pt/FC-10). Nevertheless, several residual FC sites still remained on the surface. Carbon atoms having F–C bonds with semiionic or ionic character were more positively charged than graphitic carbon, and accessible positive carbon centers may have served as Lewis acid sites, thereby enhancing chemisorption of ammonia and activation of ammonia to oxidation by O_2. Experiments using FC-28 (17) and FC-65 supports alone as catalysts showed that FC-28 exhibited weak NO/NH_3 activity at temperatures higher than 200°C, while FC-65 showed no activity under similar conditions. These results indicated that the surface of FC-28 includes some acidic sites, but that is not the case for FC-65.

To quantify the effect of fluorine content on selectivity, product selectivity based on the mass balance for N in the feed and product streams is expressed as

$$N_2\ \text{Selectivity}\,(\%) = \frac{2[N_2]}{[NO + NH_3]_{\text{initial}} - [NO + NH_3]_{\text{final}}} \times 100.$$

The product selectivity can be defined similarly for N_2O and NO_2.

Pt/FC catalysts showed higher selectivity to N_2 than the fluorine-free counterparts, Pt/FC-0 and Pt/AC, especially in the temperature range 150–200°C where Reactions [1] and [2] predominated and selectivity to NO_2 was less than 5% for all catalysts (Fig. 7). It can be seen that selectivity to N_2 was significantly improved and selectivity to N_2O was suppressed over Pt/FC catalysts when compared with fluorine-free Pt/FC-0 and Pt/AC. Compared to the fluorine-free Pt/FC-0 catalyst, it was found that using Pt/FC-10 catalysts increased N_2 selectivity by about fivefold at 150°C and about twofold at 175°C and correspondingly decreased N_2O selectivity (Fig. 7). The optimum activity and selectivity for reaction of NO with NH_3 over Pt/FC catalysts was found to be Pt/FC-28. The catalytic activity for Pt/FC-65 was inhibited by the increased fluorine content, and resulting envelopment of Pt, and selectivity to N_2 was poor. At 200°C, N_2 selectivity over Pt/FC-28 was about 2.6-fold higher than that over Pt/FC-0, and about 4.2-fold higher than that over Pt/AC.

N_2 formation in the reaction of NO with NH_3 over Pt catalysts involves dissociative chemisorption of NO at

active sites (5, 9). XPS results showed a −0.1 to −0.2 eV binding energy shift of Pt $4f_{7/2}$ for Pt/FC-10 and FC-28 compared with that of Pt/FC-0, due to the electronic interaction between FC and Pt. The increased electron density on Pt promoted dissociative chemisorption of NO by enhanced availability of electrons for donation to antibonding orbitals of NO (10), which in turn promoted activation of the NO bond. N_2O formation over fluorinated Pt/FC catalysts was suppressed when compared with that of Pt/FC-0, at temperatures below 200°C. These results are consistent with the interpretation that N_2 formation under mild conditions (Reaction [1]) was more favorable with Pt/FC catalysts.

CONCLUSIONS

A strong electronic interaction exists between F and C in both fluorinated carbon (FC) supports and the corresponding Pt/FC catalysts. The F–C bond has strong ionic character for supports having 10–28% F. The bond structure is more complex when the fluorine content is 65%. Pt in Pt/FC catalysts is more electron rich than Pt supported on fluorine-free supports, due to electron transfer from FC to Pt.

The type of carbon (FC; AC) and the fluorine content of fluorinated carbon each affect the catalyst–support interaction and thereby affect the catalytic activity and selectivity. Optimum activity and selectivity are found for Pt/FC catalysts when the support has 28% fluorine content. Beyond this fluorine level, catalytic activity is inhibited due to blocking of Pt sites caused by envelopment by the support. The promoting effect of fluorine on catalytic activity and selectivity is attributed to enhanced availability of electrons from electron-rich Pt sites, which donate electrons to NO antibonding orbitals and thereby promote dissociative chemisorption and reaction of NO.

ACKNOWLEDGMENT

We gratefully acknowledge financial support from Agrium–Carseland Nitrogen Operations, Calgary, Canada.

REFERENCES

1. Heck, R. M., *Catal. Today* **53**, 519 (1999).
2. Heck, R. M., and Farrauto, R. J., *in* "Catalytic Air Pollution Control—Commercial Technology," p. 161. Van Nostrand Princeton, NJ, 1995.
3. Radojevic, M., *Environ. Pollut.* **102**(S1), 685 (1998).
4. Forzatti, P., *Catal. Today* **62**, 51 (2000).
5. Busca, G., Lietti, L., Ramis, G., and Berti, F., *Appl. Catal. B* **18**, 1 (1998).
6. Armor, J. N., *Environ. Catal.* **552**, 172 (1996); Armor, J. N., *Environ. Catal.* **552**, 205 (1996).
7. Acke, F., and Skoglundh, M., *Appl. Catal. B* **20**, 235 (1999).
8. Takami, A., Takemoto, T., Iwakuni, H., Yamada, K., Shigetsu, M., and Komatsu, K., *Catal. Today* **35**, 75 (1997).
9. Acke, F., and Skoglundh, M., *Appl. Catal. B* **20**, 133 (1999).
10. Yentekakis, I. V., Konsolakis, M., Lambert, R. M., Macleod, N., and Nalbantian, L., *Appl. Catal. B* **22**, 123 (1999).
11. Shia, G. A., and Mani, G., *in* "Organofluorine Chemistry: Principles and Commercial Applications" (R. E. Banks, Ed.), p. 483. Plenum, New York, 1994.
12. Nanse, G., Papirer, E., Fioux, P., Moguet, F., and Tressaud, A., *Carbon* **35**, 175 (1997).
13. Tressaud, A., Moguet, F., Flandrois, S., Chambon, M., Guimon, C., Nanse, G., Papirer, E., Gupta, V., and Bahl, O. P., *J. Phys. Chem. Solids* **57**, 745A (1996).
14. Nikolenko, Y. M., and Ziatdinov, A. M., *Mol. Cryst. Liq. Cryst.* **340**, 399 (2000).
15. Tougara, H., and Okino, F., *Carbon* **38**, 241 (2000).
16. Shirasaki, T., Moguet, F., Lozano, L., Tressard, A., Nanse, G., and Papirer, E., *Carbon* **37**, 1891 (1999).
17. An, W. Z., Zhang, Q. L., Chuang, K. T., and Sanger, A. R., *Ind. Eng. Chem. Res.* **41**, 27–31.
18. Spagnolo, D., Ph.D. thesis. Department of Chemical Engineering, University of Alberta, 1997.
19. Dwyer, D. J., Robbins, J. L., Cameron, S. D., Dudash, N., and Hardenbergh, J., *ACS Symp. Ser.* **298**, 21 (1986).
20. Tauster, S. J., *ACS Symp. Ser.* **298**, 1 (1986).
21. Muniz, J., Marban, G., and Fuertes, A. B., *Appl. Catal. B* **27**, 27 (2000).
22. Krishnan, A. T., and Boehman, A. L., *Appl. Catal. B* **18**, 189 (1998).